

Sterile neutrino Dark Matter in the minimal Dirac Seesaw

J. Adhikary,^{1,*} A. Batra,^{2,†} K. Deka,^{1,‡} and F. R. Joaquim^{2,§}

¹*National Centre for Nuclear Research, Pasteura 7, Warsaw, PL-02-093, Poland*

²*Departamento de Física and CFTP, Instituto Superior Técnico, Universidade de Lisboa, Av. Rovisco Pais 1, 1049-001 Lisboa, Portugal*

We study sterile neutrino dark matter in a minimal Type-I Dirac seesaw framework where the states responsible for generating Dirac neutrino masses at tree level can be viable dark matter candidates. A \mathcal{Z}_6 symmetry, spontaneously broken to a residual \mathcal{Z}_3 by the vacuum expectation value of a singlet scalar, forbids Majorana mass operators and ensures neutrino Diracness. The lightest sterile neutrino is produced non-thermally via freeze-in from decays of Standard Model particles and an additional scalar state. We show that the presence of an additional right-handed mixing angle, θ_R , opens up viable regions of parameter space where the observed dark matter relic abundance can be reproduced while maintaining cosmological stability. This mainly stems from the absence of X-ray astrophysical constraints in our scenario. We further find that the freeze-in production of right-handed neutrinos yields a negligible contribution to ΔN_{eff} , consistent with current cosmological bounds.

I. INTRODUCTION

The Standard Model (SM) of particle physics provides a remarkably accurate description of fundamental interactions and has been validated by a wide range of experimental results. Nevertheless, it is widely recognized as an incomplete theory, as it does not incorporate mechanisms to explain two empirically established phenomena: the generation of non-zero neutrino masses [1, 2] and the existence of cosmologically stable dark matter (DM) [3, 4]. A minimal and theoretically well-motivated extension to address the first issue is the Type-I seesaw mechanism [5–10], which introduces heavy right-handed (sterile) neutrinos. Through their interaction with the SM, these states generate naturally small masses for the active neutrinos via the seesaw relation. Within this same framework, the lightest sterile neutrino can also account for the observed DM relic abundance. In this case, its production occurs via the freeze-in mechanism, characterizing it as a Feebly Interacting Massive Particle (FIMP) dark matter candidate.

In the minimal scenario, sterile neutrinos are produced non-thermally in the early Universe via their mixing with SM active neutrinos. This process, known as the Dodelson–Widrow (DW) scenario [11], arises from the small but finite probability for active neutrinos in the thermal plasma to oscillate into sterile states. As the Universe expands and cools, this out-of-equilibrium production gradually builds up a relic population of sterile neutrinos. The resulting cosmological abundance is controlled primarily by two parameters: the sterile neutrino mass and the active–sterile mixing angle. Reproducing the observed dark matter relic density inferred by the Planck satellite, $0.1126 < \Omega h^2 < 0.1246$ [4], typically requires sterile neutrino masses in the keV range and highly suppressed mixing angles.

However, this minimal framework is subject to severe phenomenological constraints. The same mixing that enables sterile neutrino production also induces radiative decays of the form $N \rightarrow \nu\gamma$ [12]. Although the corresponding lifetime typically exceeds the age of the Universe, these decays would give rise to a monochromatic X-ray line potentially observable in astrophysical data. The absence of such signals in current X-ray observations places stringent upper bounds on the active–sterile mixing angle [13–19]. When combined with independent constraints from structure

* vyotismita.adhikary@ncbj.gov.pl

† aditya.batra@tecnico.ulisboa.pt

‡ kishan.deka@ncbj.gov.pl

§ filipe.joaquim@tecnico.ulisboa.pt

formation, these limits effectively exclude the region of parameter space in which the DW scenario accounts for the entire dark matter abundance.

Despite these challenges, sterile neutrinos remain attractive dark matter candidates due to the simplicity of the underlying framework. This has motivated the exploration of alternative production scenarios. A well-known example is the Shi–Fuller mechanism [20], where resonant active–sterile oscillations occur in the presence of a large lepton asymmetry in the early Universe. This mechanism relaxes the constraints on the mixing angle, but typically requires a significant degree of degeneracy among heavy sterile neutrinos. Other possibilities include scenarios with neutrino self-interactions [21–23], production from the decay of singlet scalar fields [24–27], and non-standard cosmological histories with late-time entropy injection that modify the relic abundance [28].

Within the conventional Type-I seesaw, sterile neutrinos can also be produced through the decays of SM gauge bosons and the Higgs boson [29]. The corresponding production rates are governed by Yukawa couplings, which simultaneously set the active–sterile mixing angles responsible for their radiative decays. Requiring the DM candidate to remain cosmologically stable, together with the stringent bounds from X-ray observations, typically forces these Yukawa couplings to be extremely small, strongly suppressing this production channel.

An alternative possibility is that neutrinos are Dirac rather than Majorana particles. The continued non-observation of neutrinoless double beta decay ($0\nu\beta\beta$) [30–32] may point in this direction, as suggested by the black-box theorem [33]. In this case, neutrino mass generation requires mechanisms that forbid Majorana mass terms, typically through additional symmetries [34]. Such constructions include Dirac realizations of the Type-I [35–38] and Type-II [39–41] seesaw mechanisms. Moreover, due to the presence of additional parameters, Dirac seesaws do not typically require extremely large mediator masses, unlike Majorana seesaw models, to ensure the smallness of neutrino masses. Hence, having sterile neutrino masses at the scale required to explain DM (~ 100 keV) is more natural. A particularly interesting feature of Dirac seesaw models is the presence of an additional mixing angle, θ_R , associated with the right-handed neutrino sector. This parameter can contribute to sterile neutrino production via Higgs decays without directly affecting the radiative decay channel probed by X-ray observations.

In this work, we propose a minimal version of the Type-I Dirac seesaw and demonstrate that the additional degree of freedom θ_R significantly relaxes X-ray constraints and opens up viable regions of parameter space for sterile neutrino dark matter. We further show that this setup provides a minimal realization of Dirac neutrino mass generation “seeded” by dark matter: the mechanism operates already at tree level, and is therefore structurally simpler than radiative constructions such as the Dirac scotogenic model [42]. This paper is organised as follows. In Sec. II we introduce a minimal realization of the Dirac seesaw model. The phenomenological implications for dark matter and cosmology are discussed in Sec. III. Finally, our conclusions are presented in Sec. IV. Additional details on the scalar sector, and relevant formulas used in the calculations are provided in the appendices.

II. THE MODEL

We extend the SM by introducing three right-handed neutrinos ν_{Ri} , three pairs of Dirac fermion fields N_i and a real singlet σ . In addition, a \mathcal{Z}_6 symmetry is imposed to protect the Dirac nature of neutrinos. Assigning the \mathcal{Z}_6 charges as shown in Table I, we forbid all effective Majorana neutrino mass generation operators of the type $(\bar{\ell}_L^c \tilde{\Phi}^*)(\tilde{\Phi}^\dagger \ell_L)\sigma^n \sigma^{*n'}$, where $\ell_L = (\nu_L, e_L^-)^T$ and $\Phi = (\phi^+, \phi^0)^T$ denote the SM lepton and Higgs doublet, respectively, and $\tilde{\Phi} = i\tau_2 \Phi$, with τ_2 being the complex Pauli matrix. $n = n' = 0$ corresponds to the well-known Weinberg operator [43]. After σ gains a vacuum expectation value (VEV)¹, the \mathcal{Z}_6 symmetry is spontaneously broken to a residual unbroken \mathcal{Z}_3 symmetry. The fields that have non-trivial charges under the \mathcal{Z}_3 symmetry transform as: $(\ell_L, e_R, \nu_R, N_{L,R}) \rightarrow \omega(\ell_L, e_R, \nu_R, N_{L,R})$. This \mathcal{Z}_3 symmetry forbids all the above Majorana type operators. The idea of using residual \mathcal{Z}_N symmetries to prevent

¹ The scalar sector is discussed in detail in Appendix A, where we present the scalar mass spectrum and mixing structure, together with the vacuum stability conditions imposed in our numerical analysis.

	Fields	$SU(2)_L \otimes U(1)_Y$	\mathcal{Z}_6
Fermions	ℓ_L	$(\mathbf{2}, -1/2)$	ω
	e_R	$(\mathbf{1}, -1)$	ω
	ν_R	$(\mathbf{1}, 0)$	ω^4
	$N_{L,R}$	$(\mathbf{1}, 0)$	ω
Scalars	Φ	$(\mathbf{2}, 1/2)$	1
	σ	$(\mathbf{1}, 0)$	ω^3

TABLE I: Field content and transformation properties under $SU(2)_L \otimes U(1)_Y$ and \mathcal{Z}_6 .

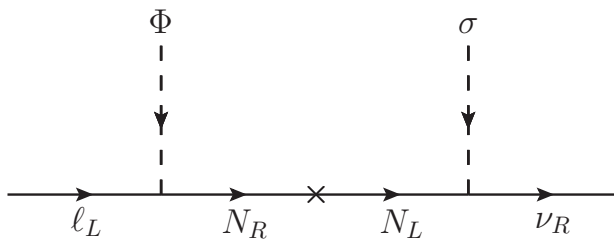


FIG. 1: Feynman diagram for tree-level Dirac neutrino mass generation with $U(1)_L$ spontaneously broken.

Majorana neutrino masses has previously been explored in the context of a $U(1)_{B-L}$ symmetry in Ref. [42]. Effective Dirac neutrino mass operators, generically expressed as, $(\bar{\ell}_L \tilde{\Phi} \nu_R) \sigma^n \sigma^{*n'}$ are allowed by the \mathcal{Z}_3 symmetry, with the lowest dimension operator being the dimension-5 $(\bar{\ell}_L \tilde{\Phi} \nu_R) \sigma$, corresponding to $n = 1, n' = 0$. The tree-level Yukawa interaction $\bar{\ell}_L \tilde{\Phi} \nu_R$ is forbidden by the \mathcal{Z}_6 symmetry.

With the field content and symmetries defined above, the Yukawa Lagrangian takes the form,

$$-\mathcal{L} = \mathbf{Y}_e \bar{\ell}_L \Phi e_R + \mathbf{Y}_\nu \bar{\ell}_L \tilde{\Phi} N_R + \mathbf{Y}_\sigma \bar{N}_L \nu_R \sigma + \mathbf{M}_N \bar{N}_L N_R + \text{H.c.}, \quad (1)$$

where the Yukawa couplings \mathbf{Y}_e , \mathbf{Y}_ν and \mathbf{Y}_σ and the bare mass \mathbf{M}_N are 3×3 matrices. The 6×6 Dirac neutrino mass matrix can be written in the basis $(\nu_L, N_L, \nu_R, N_R)^T$ as,

$$\mathcal{M}_{\nu, N} = \begin{pmatrix} 0 & \mathbf{Y}_\nu v_\phi / \sqrt{2} \\ \mathbf{Y}_\sigma v_\sigma / \sqrt{2} & \mathbf{M}_N \end{pmatrix}, \quad (2)$$

where v_ϕ and v_σ are the VEVs of the Higgs field Φ and the real singlet σ respectively. In the limit $M_{N_{ij}} \gg v_\phi, v_\sigma$, the effective 3×3 mass matrix for the active neutrinos is approximately given by [44],

$$\mathbf{M}_\nu \simeq \frac{v_\phi v_\sigma}{2} \mathbf{Y}_\nu \mathbf{M}^{-1} \mathbf{Y}_\sigma. \quad (3)$$

The rotation to the neutrino mass-eigenstate basis can be defined as,

$$(\nu_e, \nu_\mu, \nu_\tau, N_e, N_\mu, N_\tau)^T_{L,R} = \mathbf{U}_{L,R} (\nu_1, \nu_2, \nu_3, N_1, N_2, N_3)^T_{L,R}, \quad (4)$$

with ν_i (N_i) denoting the physical active (sterile) Dirac neutrino states. For the sake of simplicity, we neglect intergenerational mixing among active and sterile neutrinos. In this case, the left and right active-sterile mixing can be parametrised by the angles θ_{Li} and θ_{Ri} , respectively. For each generation, these are given as,

$$\tan(2\theta_{Li}) = \frac{2\sqrt{2}M_{N_i}Y_{\nu_i}v_\phi}{Y_{\sigma_i}v_\sigma^2 + 2M_{N_i}^2 - Y_{\nu_i}v_\phi^2}, \quad \tan(2\theta_{Ri}) = \frac{2\sqrt{2}M_{N_i}Y_{\sigma_i}v_\sigma}{Y_{\nu_i}v_\phi^2 + 2M_{N_i}^2 - Y_{\sigma_i}v_\sigma^2} \quad (i = 1, 2, 3), \quad (5)$$

where the Y 's and M_N 's are the diagonal elements of the corresponding matrices.

Before moving on to the phenomenology of the model, it is worth commenting on the choice of the number of species of $N_{L,R}$ and ν_R . In the Dirac seesaw, it is possible to correctly reproduce the observed neutrino oscillation data with

only two species of $N_{L,R}$ and ν_R each. This would lead to one massless active neutrino. However, the experimentally measured solar mass-squared difference Δm_{12}^2 would place a very tight constraint on the mass of the lightest sterile neutrino and on the mixing angles $\theta_{L1,R1}$. In fact, the resulting available parameter space would already be excluded by X-ray searches of the radiative decay of a sterile neutrino $N \rightarrow \nu\gamma$ which highly constrains the mass and mixing angle of the sterile neutrino (see Sec. III A for details). Therefore, in this work, we consider three species of $N_{L,R}$ and ν_R each.

III. PHENOMENOLOGY

In this section, we study the phenomenological implications of our model for DM and the effective number of relativistic degrees of freedom, N_{eff} . We perform a numerical scan over the mixing angles $\theta_{L1,R1}$ and the mass of the dark matter candidate M_{N_1} . The SM Higgs boson mass is fixed to its experimentally measured value $m_h = 125.20 \text{ GeV}$ [45], and we choose $m_H = 500 \text{ GeV}$, $\alpha = 0.1$, and $v_\sigma = 150 \text{ GeV}$. The scalar couplings are determined by eqs. (A6) given in Appendix A, where we also present the scalar mass spectrum and mixing, together with the vacuum stability conditions imposed in our numerical analysis. For simplicity, we assume the Yukawa couplings to be real and extract their values using eq. (5).

A. Dark matter relic abundance

In the present framework, the lightest sterile neutrino N_1 is very weakly coupled to the SM and is a viable DM candidate through a freeze-in mechanism. Its production occurs via the following dominant decay processes:

$$W^+ \rightarrow N_1 e_i^+, \quad W^- \rightarrow \bar{N}_1 e_i^-, \quad Z \rightarrow N_1 \bar{N}_1, \quad h/H \rightarrow N_1 \bar{\nu}_1, \quad h/H \rightarrow \bar{N}_1 \nu_1, \quad (6)$$

where h and H are the physical scalars explicitly defined in Appendix A. In our Dirac seesaw model, the interactions involving these scalars stem from the Yukawa terms $\mathbf{Y}_\sigma \bar{N}_L \nu_R \sigma$ and $\mathbf{Y}_\nu \bar{\ell}_L \tilde{\Phi} N_R$, which, in the mass basis read:

$$-\mathcal{L}_{\text{int}} = \frac{1}{\sqrt{2}} \sum_{j,l=1}^6 \sum_{i=1}^3 \sum_{k=4}^6 \left[\mathbf{U}_L^{*ji} \mathbf{U}_R^{kl} (h c_\alpha + H s_\alpha) \mathbf{Y}_\nu^{i,k-3} + \mathbf{U}_L^{*jk} \mathbf{U}_R^{il} (-h s_\alpha + H c_\alpha) \mathbf{Y}_\sigma^{k-3,i} \right] \bar{\nu}_{jL} \nu_{lR} + \text{H.c.}, \quad (7)$$

with $\mathbf{U}_{L,R}$ as defined in eq. (4) and α being the scalar mixing angle given in eq. (A5). From now on, ν_{1-3} (ν_{4-6}) denote the active (sterile) Dirac neutrino mass eigenstates. Thus, fixing $j, l = 4$ leads to terms involved in the production of the lightest sterile neutrino N_1 .

Besides the freeze-in decays given in eq. (6), there can also be contribution to the production of N_1 from the DW mechanism, namely [46],

$$\Omega_{\text{DW}} h^2 \simeq 0.3 \times \left[\frac{\sin^2(2\theta_{L1})}{10^{-10}} \right] \left(\frac{m_s}{100 \text{ keV}} \right)^2, \quad (8)$$

where m_s corresponds here to the mass of N_1 , i.e. $m_s = M_{\nu_4} \simeq M_{N_1}$. In our case, to obtain the correct observed relic density, θ_{L1} must be $\sim 10^{-9}$ when $m_s \sim 10^{-4} \text{ GeV} = 100 \text{ keV}$. For these parameter choices, the corresponding DW contribution to the relic density is $\sim 10^{-8}$ being, therefore, negligible.

The way we compute the relic abundance of the sterile fermion N_1 is by numerically solving the Boltzmann equation for its comoving number density,

$$\frac{dY_{N_1}}{dz} = \frac{2M_{\text{Pl}}}{1.66 m_h^2} \frac{z \sqrt{g_*(T)}}{g_{*s}(T)} \sum_i \langle \Gamma_i \rangle (Y_i^{\text{eq}} - Y_{N_1}), \quad (9)$$

where $z \equiv m_h/T$, $g_*(T)$ and $g_{*s}(T)$ denote the effective relativistic degrees of freedom for the energy and entropy densities, respectively. The expressions for the thermally-averaged decay widths $\langle \Gamma_i \rangle$ for the various modes were taken

Decay channel	θ_L -dominated	θ_R -dominated
W^\pm	~ 1	~ 0
Z	~ 0	~ 0
H	~ 0	~ 0.44
h	~ 0	~ 0.56

TABLE II: Relative contributions of individual decay channels to the DM relic density for two benchmark points. The θ_L -dominated column corresponds to $M_{N_1} = 9.98 \times 10^{-4}$ GeV, $\theta_{L1} = 3.95 \times 10^{-9}$ and $\theta_{R1} = 10^{-10}$ with a total relic density of $\Omega h^2 = 0.1211$. For the θ_R -dominated case, $M_{N_1} = 9.82 \times 10^{-2}$ GeV, $\theta_{R1} = 1.76 \times 10^{-6}$ and $\theta_1 = 10^{-15}$, leading to $\Omega h^2 = 0.1128$.

from [47]. In the case of h and H decays, the final states are $N_1 \bar{\nu}_1$ and $\bar{N}_1 \nu_1$ instead of $N_1 \bar{N}_1$. Annihilation channels mediated by h , H and Z are suppressed by the fourth power of the mediator mass ($\sim m^4$) compared to decay channels. Therefore, their contribution to relic density in our case is negligible and hence neglected. The equilibrium yield for a generic particle species i of mass m_i and internal degrees of freedom g_i is taken to be,

$$Y_i^{\text{eq}}(z) = \frac{45}{4\pi^4} \frac{g_i}{g_{*s}(T)} \left(\frac{m_i}{m_h} z \right)^2 K_2 \left(\frac{m_i}{m_h} z \right). \quad (10)$$

The Boltzmann equation (9) is solved numerically and the final yield at late times is converted into the present-day relic density via

$$\Omega_{N_1} h^2 = 2.755 \times 10^8 \left(\frac{M_{N_1}}{\text{GeV}} \right) Y_{N_1}(T_{\text{present}}), \quad (11)$$

where, $Y_{N_1}(T_{\text{present}})$ represents the comoving density of DM at present time. In our numerical scan, we apply the following constraints:

- Perturbativity of scalar couplings ($\lambda_\Phi, \lambda_\sigma, \lambda_{\Phi\sigma} \leq 4\pi$) and Yukawa couplings ($Y_{\nu_1}, Y_{\sigma_1} \leq \sqrt{4\pi}$).
- Sum of neutrino masses ≤ 0.12 eV, a constraint obtained from the observations of the CMB, combined with lensing and baryon acoustic oscillations data [45].
- Non-thermality condition: the rate of production of N_1 is less than the expansion rate of the Universe at a temperature $T \sim M$, where M is the mass of the decaying particle [48]. That is, $\Gamma/H < 1$, where Γ is the decay width and H is the Hubble parameter.
- The sterile neutrino N_1 can decay into SM fermions depending on its mass. Namely:
 - For $m < 2m_e$, the dominant decay channel is $N_1 \rightarrow \nu_1 \nu_i \bar{\nu}_i$, where $i = 1, 2, 3$. This decay is mediated by virtual Z , h and H bosons. The h and H mediated decay widths are much suppressed compared to the Z [49].
 - For $m \geq 2m_e$, the decay $N_1 \rightarrow \nu_1 e^+ e^-$ opens up. This decay is mediated by virtual W , Z , h and H bosons. However, this decay width is much smaller compared to $N_1 \rightarrow \nu_1 \nu_i \bar{\nu}_i$.
 - For $m \geq 100$ MeV, several possibilities open up, including hadronic decay modes [50], therefore we have considered sterile neutrino masses upto 100 MeV.

We require these decays to be suppressed so that the lifetime of N_1 and \bar{N}_1 is longer than the age of the Universe, $t_{\text{Universe}} = 4.4 \times 10^{17}$ s.

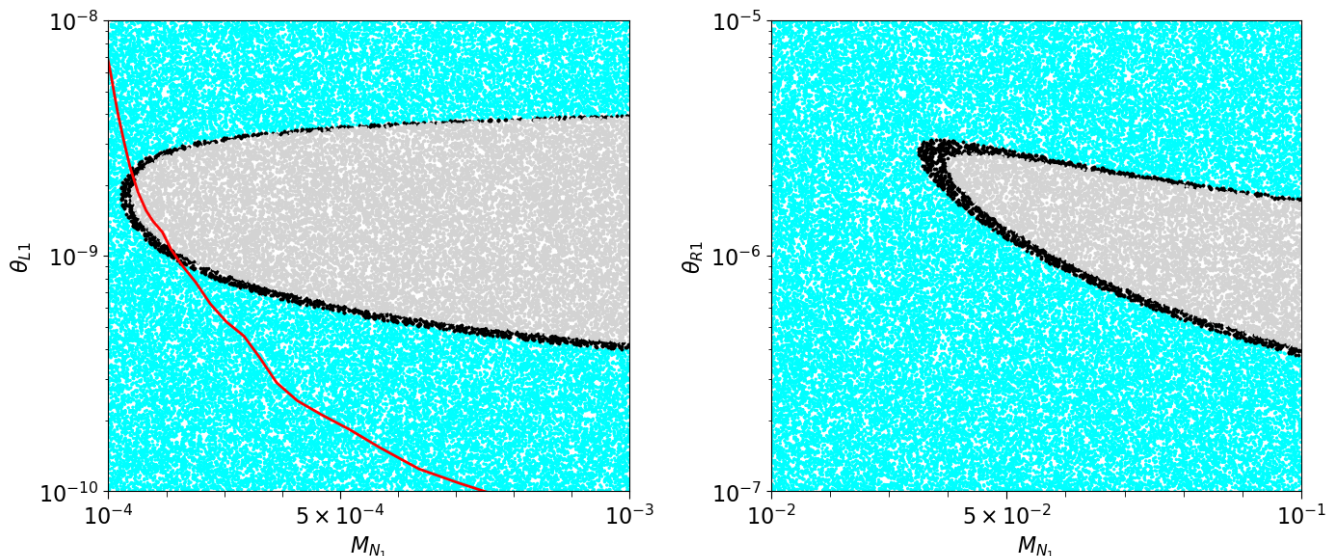


FIG. 2: Left: Parameter space in the (M_{N_1}, θ_{L1}) plane obtained from the numerical scan fixing $\theta_R = 10^{-10}$. The blue points are underabundant ($\Omega h^2 < 0.1126$), black points are cosmologically viable ($0.1126 < \Omega h^2 < 0.1246$), and grey points are overabundant ($\Omega h^2 > 0.1246$). The red curve indicates the X-ray constraint, with the region above it excluded. Right: Correlation between the right-handed mixing angle θ_{R1} and the sterile fermion mass M_{N_1} fixing $\theta_L = 10^{-15}$. Colour scheme is the same for both plots.

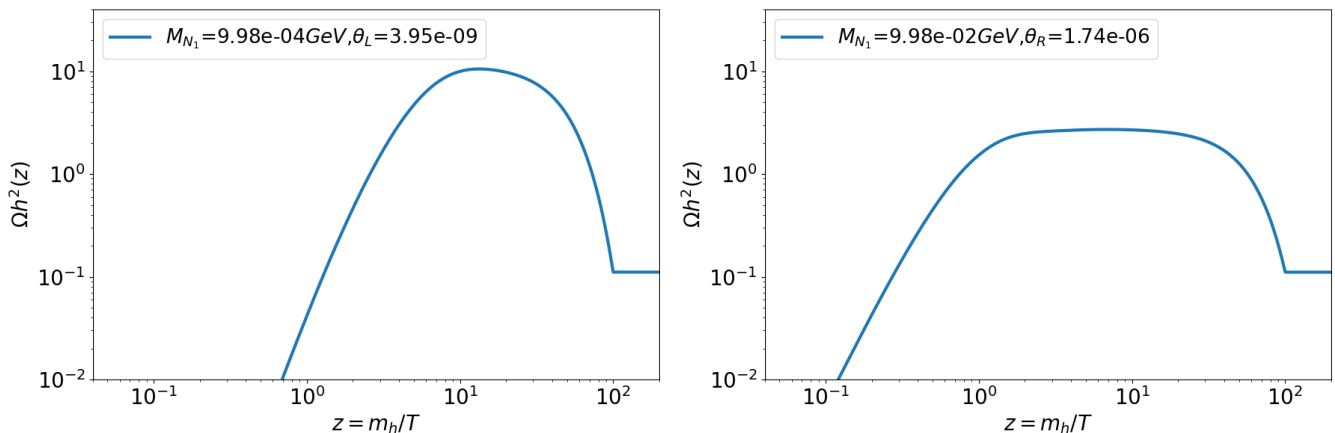


FIG. 3: Left: The evolution of the relic abundance is shown as a function of z corresponding to $M_{N_1} = 9.98 \times 10^{-4}$ GeV, $\theta_{L1} = 3.95 \times 10^{-9}$ and $\theta_{R1} = 10^{-10}$. Right: The evolution of the relic abundance is shown as a function of z corresponding to $M_{N_1} = 9.82 \times 10^{-2}$ GeV, $\theta_{R1} = 1.76 \times 10^{-6}$ and $\theta_{L1} = 10^{-15}$. For both cases, the displayed trajectory corresponds to the parameter point with the largest drop from its peak value, highlighting the effect of inverse processes that partially deplete the dark matter abundance at later times.

In Fig. 2 we show the results of our parameter scan. The blue points correspond to underabundant DM ($\Omega h^2 < 0.1126$), the grey points to overabundant ($\Omega h^2 > 0.1246$) and the black points are cosmologically viable ($0.1126 < \Omega h^2 < 0.1246$), as inferred from Planck satellite data at the 3σ level [4]. In the left panel, we show the parameter space in the (M_{N_1}, θ_{L1}) plane fixing θ_R to a very small value, $\theta_R = 10^{-10}$, so that DM is entirely produced through interactions involving θ_L . The region above the red line is excluded by X-ray astrophysical searches. From Table II, where the relative contribution from different decay channels producing N_1 is shown for comparison, we can see

that the dominant production channel is the W^\pm decay. The results show that X-rays exclude almost the entire DM-allowed parameter space with masses larger than $\sim 10^{-4}$ GeV. The right panel shows the parameter space in the (M_{N_1}, θ_{R1}) plane choosing $\theta_L = 10^{-15}$. In this case, DM is entirely produced through interactions involving θ_R (see Table II), h and H decays being the dominant production channels. These are usually suppressed in Majorana sterile neutrino DM models due to the tight constraint on the mixing angle. However, in our Dirac seesaw framework, these decays can be enhanced by θ_R . Since the decay $N \rightarrow \nu\gamma$ occurs through a W loop, θ_R remains unconstrained from X-ray observations. Hence, it is possible to obtain the correct DM relic density even for comparatively large mass scales.

In addition to the production channels, the Boltzmann equation also includes the corresponding inverse processes, which give rise to back-reaction effects. These appear through terms proportional to $(Y_i^{\text{eq}} - Y_{N_1})$ for the decay processes. At early times, when DM abundance satisfies $Y_{N_1} \ll Y^{\text{eq}}$, these contributions are positive and DM production proceeds efficiently through decays of particles in the thermal bath. As the abundance of N_1 increases, the corresponding inverse reactions, such as $N_1 + \nu \rightarrow h, H$ and $N_1 + \bar{\nu} \rightarrow h, H$, become progressively more relevant. These processes partially deplete the dark matter abundance and reduce the net production rate. As a consequence, the evolution of the relic abundance may exhibit a peak followed by a mild decrease before eventually approaching a constant value at late times. The peak typically appears at $z \sim \mathcal{O}(10\text{--}100)$, when the temperature of the thermal bath drops below the masses of the particles responsible for the dominant production channels. In this regime, the equilibrium number densities of these particles become Boltzmann suppressed, leading to a rapid reduction in the production rate. At the same time, inverse processes start to partially counteract the accumulated abundance, producing a small depletion before the yield ultimately freezes to its asymptotic value.

Two examples of the aforementioned behaviour are shown in Fig. 3. In the left panel, the relic abundance is shown as a function of z , for a benchmark point from the left panel of Fig. 2 with a sizable θ_L and keeping $\theta_R = 10^{-10}$, illustrating the effect of the left-handed mixing on freeze-in production. Conversely, the right panel shows the evolution for a benchmark point from the right panel of Fig. 2 when θ_R is sizable while fixing $\theta_L = 10^{-15}$, thereby isolating the effect of the right-handed mixing. In both cases, the relic abundance initially increases as dark matter particles are gradually produced from the thermal bath through freeze-in processes. As the temperature decreases and the abundance grows, inverse reactions become increasingly relevant and partially counteract the production rate. This leads to a mild decrease in the abundance after it reaches its peak before eventually approaching a constant value at late times.

In conclusion, for the model considered here, the dominant contributions arise from decay channels such as $h, H \rightarrow \bar{N}_1\nu$ and $h, H \rightarrow N_1\bar{\nu}$, as well as processes involving electroweak gauge bosons, including $W^+ \rightarrow N_1 e_i^+$, $W^- \rightarrow \bar{N}_1 e_i^-$, and $Z \rightarrow N_1 \bar{N}_1$. The relative importance of these channels is controlled by the mixing angles θ_L and θ_R , which determine the strength of the interaction between the dark sector and the SM bath.

B. Contribution to N_{eff} from ν_R production

Since we are working in a Dirac neutrino framework, the light right-handed neutrinos ν_R contribute as additional relativistic species, thereby modifying the effective number of relativistic degrees of freedom in the early Universe, denoted as N_{eff} . This quantity is highly constrained from current cosmic microwave background observations [51]. Here we compute the contribution to the effective number of relativistic neutrino species ΔN_{eff} , coming from ν_R production, which do not thermalise in the early Universe and are instead generated via freeze-in. Their production channels and corresponding squared decay amplitudes $|\mathcal{M}|^2$ are:

$$\begin{aligned} h \rightarrow \bar{N}_{L_i} \nu_{R_i} : \quad & |\mathcal{M}|^2 = 2g_{h\bar{N}_i\nu_i}^2 [m_h^2 - (m_{N_i} + m_{\nu_i})^2], \\ H \rightarrow \bar{N}_{L_i} \nu_{R_i} : \quad & |\mathcal{M}|^2 = 2g_{H\bar{N}_i\nu_i}^2 [m_H^2 - (m_{N_i} + m_{\nu_i})^2]. \end{aligned} \quad (12)$$

where $g_{H\bar{N}_i\nu_i}$ and $g_{h\bar{N}_i\nu_i}$ are given in eq. (B1). To compute ΔN_{eff} in freeze-in regime, we follow the method presented in Ref. [52]. The Boltzmann equations for the new ν_R -SM interactions are given as [52, 53],

$$\dot{\rho}_{\nu_R} + 4 \left(\frac{\dot{a}}{a} \right) \rho_{\nu_R} = C_{\nu_R}, \quad (13)$$

$$\dot{\rho}_{\text{SM}} + 3 \left(\frac{\dot{a}}{a} \right) (\rho_{\text{SM}} + p_{\text{SM}}) = -C_{\nu_R}, \quad (14)$$

where a is the cosmological scale factor, ρ_{SM} and ρ_{ν_R} are the energy densities of SM particles and ν_R , respectively, p_{SM} is the pressure term of SM particles and C_{ν_R} denotes the collision term for the ν_R -SM interaction. The collision term for the $1 \rightarrow 2$ process that we consider for ν_R production can be written as,

$$C_{\nu_R} = N_{\nu_R} \int E_{\nu_R} \left(\prod_i \frac{1}{(2\pi)^3} \frac{d^3 p_i}{2E_i} \right) \delta^4(p_1 - p_2 - p_3) |\mathcal{M}|^2 \left(\frac{1}{\exp(E_1/T_1) - 1} \right). \quad (15)$$

Here, $N_{\nu_R} = 6$ is the number of ν_R ($\bar{\nu}_R$) flavours; E_{ν_R} is the energy of ν_R ; p_i , E_i and T_i are the momentum, energy and temperature of the i -th particle. $|\mathcal{M}|^2$ denotes the squared decay amplitude of the $1 \rightarrow 2$ processes whose expressions are given in eq. (12).

We solve the Boltzmann eqs. (13) and (14) numerically using a Monte-Carlo integration code² [52]. The contribution of ν_R to N_{eff} is by definition,

$$\Delta N_{\text{eff}} = \frac{8}{7} \left(\frac{11}{4} \right)^{4/3} \frac{\rho_{\nu_R,0}}{\rho_{\gamma,0}}. \quad (16)$$

where $\rho_{\nu_R,0}$ and $\rho_{\gamma,0}$ are the energy densities of ν_R and photons at some time after e^\pm -annihilation. We can rewrite this in terms of the corresponding temperature ratios at $T_{SM} = 10$ MeV as [52, 53],

$$\Delta N_{\text{eff}} = N_{\nu_R} \left(\frac{T_{\nu_R,10}}{T_{\gamma,10}} \right). \quad (17)$$

In our case, we obtain no significant contributions to ΔN_{eff} ($\sim 10^{-17}$) for typical values of the masses of N_1 and H and couplings of the interactions, considered in the parameter space of Fig. 2. This is consistent with the results shown in Ref. [52] for a similar case.

IV. SUMMARY AND OUTLOOK

In this work, we have presented a minimal model where Dirac neutrino masses are ‘‘seeded’’ by DM. In particular, we show that the lightest sterile neutrino that mediates neutrino mass generation at tree-level via the Dirac seesaw mechanism can simultaneously serve as viable DM candidate. The Dirac nature of neutrinos is enforced by a \mathcal{Z}_6 symmetry that is spontaneously broken to a residual \mathcal{Z}_3 symmetry once a real singlet scalar σ acquires a vacuum expectation value. This residual symmetry forbids all Majorana neutrino mass operators, thereby ensuring that neutrinos remain Dirac particles.

We considered the minimal particle content capable of producing a phenomenologically viable dark matter scenario, consisting of three generations of $N_{L,R}$ and ν_R . A setup with only two generations, which would predict one massless active neutrino, is excluded by X-ray constraints arising from the radiative decay channel $N \rightarrow \nu\gamma$. Focusing on the lightest sterile neutrino N_1 as the dark matter candidate, we studied its non-thermal production via freeze-in from the decays of SM particles as well as the additional scalar H . At the same time, we ensured that the lifetime of N_1 exceeds the age of the Universe, rendering it effectively stable on cosmological timescales. Our parameter scan reveals two

² <https://github.com/xuhenglou/Thermal.Boltzmann.Solver>

qualitatively distinct regimes. When production processes controlled by the left-handed mixing angle θ_L dominate, the allowed parameter space is strongly constrained by X-ray observations, leading to viable dark matter masses in the lower mass range ($M_{N_1} \sim 10^{-4}$ GeV). In contrast, when production is governed primarily by the right-handed mixing angle θ_R , the X-ray limits are absent, since θ_R does not contribute to the $N \rightarrow \nu\gamma$ decay. This allows for viable dark matter at higher sterile neutrino masses ($M_{N_1} > 10^{-2}$ GeV). We also examined the cosmological implications of the model, in particular the contribution to the effective number of relativistic species, ΔN_{eff} . We find that the freeze-in production of right-handed neutrinos ν_R yields a negligible contribution across the entire parameter space, ensuring consistency with current cosmic microwave background constraints [51].

Overall, our setup provides the simplest framework in which a *dark*-sector induces non-zero Dirac neutrino masses. Several alternative approaches have been explored in the literature. For instance, Refs. [37, 54] studied scalar dark matter in the context of Dirac seesaw frameworks, while Ref. [55] considered $SU(2)_L$ doublet sterile neutrinos as weakly interacting massive particle (WIMP) dark matter produced through freeze-out. Another possibility involves extending the gauge sector with a $U(1)_{B-L}$ symmetry and an additional Z' boson [56]. These scenarios lead to distinct phenomenological and cosmological signatures, particularly in relation to dark matter production mechanisms and potential contributions to ΔN_{eff} .

ACKNOWLEDGMENTS

We thank Rahul Srivastava for valuable discussions and Dhanashree Pathe for help with the numerical code. J.A. is supported by the National Science Centre, Poland (research grant No. 2021/42/E/ST2/00031). The work of K.D. is partially supported by the grant BPI/STE/2021/1/00033/U/00001. A.B. is supported by the PhD grant UI/BD/154391/2023 from the Fundação para a Ciência e a Tecnologia (FCT, Portugal). The work of A.B. and F.R.J. is also supported by the [FCT project UID/00777/2025](#).

Appendix A: Scalar sector

As shown in Table I, the scalar sector of our model contains the SM Higgs doublet Φ and a real singlet σ , which we define as,

$$\Phi = \begin{pmatrix} \phi^+ \\ \phi^0 \end{pmatrix} = \frac{1}{\sqrt{2}} \begin{pmatrix} \sqrt{2}\phi^+ \\ v_\phi + \phi_R + i\phi_I \end{pmatrix}; \quad \sigma = \frac{v_\sigma + \sigma_R}{\sqrt{2}}. \quad (\text{A1})$$

The most general scalar potential is given by,

$$V = m_\Phi^2 (\Phi^\dagger \Phi) + m_\sigma^2 \sigma^2 + \frac{\lambda_\Phi}{2} (\Phi^\dagger \Phi)^2 + \frac{\lambda_\sigma}{2} \sigma^4 + \lambda_{\Phi\sigma} (\Phi^\dagger \Phi) \sigma^2. \quad (\text{A2})$$

To ensure that it is bounded from below, the quartic couplings must fulfill the conditions [57],

$$\lambda_\Phi \geq 0, \quad \lambda_\sigma \geq 0, \quad \text{and} \quad \lambda_{\Phi\sigma} \geq -\sqrt{\lambda_\Phi \lambda_\sigma}. \quad (\text{A3})$$

There are two neutral CP-even Higgs scalars h and H (from the mixing between ϕ_R and σ_R) with masses

$$m_{h,H}^2 = \frac{1}{2} \left(v_\phi^2 \lambda_\Phi + v_\sigma^2 \lambda_\sigma \pm \sqrt{\left(v_\sigma^2 \lambda_\sigma - v_\phi^2 \lambda_\Phi \right)^2 + 4v_\phi^2 v_\sigma^2 \lambda_{\Phi\sigma}^2} \right). \quad (\text{A4})$$

The h and H mass eigenstates are related to ϕ_R and σ_R through the 2×2 orthogonal matrix:

$$\begin{pmatrix} h \\ H \end{pmatrix} = \begin{pmatrix} \cos \alpha & -\sin \alpha \\ \sin \alpha & \cos \alpha \end{pmatrix} \begin{pmatrix} \phi_R \\ \sigma_R \end{pmatrix}, \quad (\text{A5})$$

where α is the mixing angle. We can express the potential terms λ_Φ , λ_σ , and $\lambda_{\Phi\sigma}$ in terms of α , m_h and m_H as follows:

$$\begin{aligned}\lambda_\Phi &= \frac{c_\alpha^2 m_h^2 + s_\alpha^2 m_H^2}{v_\phi^2}, \\ \lambda_\sigma &= \frac{s_\alpha^2 m_h^2 + c_\alpha^2 m_H^2}{v_\sigma^2}, \\ \lambda_{\Phi\sigma} &= \frac{c_\alpha s_\alpha (m_H^2 - m_h^2)}{v_\phi v_\sigma},\end{aligned}\tag{A6}$$

where $c_\alpha = \cos \alpha$ and $s_\alpha = \sin \alpha$.

Appendix B: Relevant interaction vertices

To find the relic density of N_1 , the cross-sections of all the dominant production processes must be computed. Their analytical expressions have been presented in Ref. [47] for a $U(1)_{B-L}$ model and can be used separately for N_1 and \bar{N}_1 here. The relevant interaction vertices for the processes given in eq. (6) are:

$$\begin{aligned}g_{h\bar{N}_1\nu_1} &= \frac{1}{\sqrt{2}}(-Y_\nu^{11} c_\alpha \sin \theta_{L1} \sin \theta_{R1} - Y_\sigma^{11} s_\alpha \cos \theta_{L1} \cos \theta_{R1}), \\ g_{H\bar{N}_1\nu_1} &= \frac{1}{\sqrt{2}}(-Y_\nu^{11} s_\alpha \sin \theta_{L1} \sin \theta_{R1} + Y_\sigma^{11} c_\alpha \cos \theta_{L1} \cos \theta_{R1}), \\ g_{hN_1\bar{\nu}_1} &= \frac{1}{\sqrt{2}}(Y_\nu^{11} c_\alpha \cos \theta_{L1} \cos \theta_{R1} + Y_\sigma^{11} s_\alpha \sin \theta_{L1} \sin \theta_{R1}), \\ g_{HN_1\bar{\nu}_1} &= \frac{1}{\sqrt{2}}(Y_\nu^{11} s_\alpha \cos \theta_{L1} \cos \theta_{R1} - Y_\sigma^{11} c_\alpha \sin \theta_{L1} \sin \theta_{R1}).\end{aligned}\tag{B1}$$

All terms proportional to the sine of the neutrino mixing angles are negligible compared to those proportional to the cosine.

-
- [1] T. Kajita, ‘‘Nobel Lecture: Discovery of atmospheric neutrino oscillations,’’ *Rev. Mod. Phys.* **88** no. 3, (2016) 030501.
 - [2] A. B. McDonald, ‘‘Nobel Lecture: The Sudbury Neutrino Observatory: Observation of flavor change for solar neutrinos,’’ *Rev. Mod. Phys.* **88** no. 3, (2016) 030502.
 - [3] G. Bertone, D. Hooper, and J. Silk, ‘‘Particle dark matter: Evidence, candidates and constraints,’’ *Phys. Rept.* **405** (2005) 279–390, [arXiv:hep-ph/0404175](#).
 - [4] **Planck** Collaboration, N. Aghanim *et al.*, ‘‘Planck 2018 results. VI. Cosmological parameters,’’ *Astron. Astrophys.* **641** (2020) A6, [arXiv:1807.06209 \[astro-ph.CO\]](#). [Erratum: *Astron. Astrophys.* 652, C4 (2021)].
 - [5] P. Minkowski, ‘‘ $\mu \rightarrow e\gamma$ at a Rate of One Out of 10^9 Muon Decays?,’’ *Phys. Lett. B* **67** (1977) 421–428.
 - [6] M. Gell-Mann, P. Ramond, and R. Slansky, ‘‘Complex Spinors and Unified Theories,’’ *Conf. Proc. C* **790927** (1979) 315–321, [arXiv:1306.4669 \[hep-th\]](#).
 - [7] T. Yanagida, ‘‘Horizontal gauge symmetry and masses of neutrinos,’’ *Conf. Proc. C* **7902131** (1979) 95–99.
 - [8] J. Schechter and J. W. F. Valle, ‘‘Neutrino Masses in $SU(2) \times U(1)$ Theories,’’ *Phys. Rev. D* **22** (1980) 2227.
 - [9] S. L. Glashow, ‘‘The Future of Elementary Particle Physics,’’ *NATO Sci. Ser. B* **61** (1980) 687.
 - [10] R. N. Mohapatra and G. Senjanovic, ‘‘Neutrino Mass and Spontaneous Parity Nonconservation,’’ *Phys. Rev. Lett.* **44** (1980) 912.
 - [11] S. Dodelson and L. M. Widrow, ‘‘Sterile-neutrinos as dark matter,’’ *Phys. Rev. Lett.* **72** (1994) 17–20, [arXiv:hep-ph/9303287](#).
 - [12] P. B. Pal and L. Wolfenstein, ‘‘Radiative Decays of Massive Neutrinos,’’ *Phys. Rev. D* **25** (1982) 766.
 - [13] A. Boyarsky, D. Malyshev, A. Neronov, and O. Ruchayskiy, ‘‘Constraining DM properties with SPI,’’ *Mon. Not. Roy. Astron. Soc.* **387** (2008) 1345, [arXiv:0710.4922 \[astro-ph\]](#).

- [14] S. Horiuchi, P. J. Humphrey, J. Onorbe, K. N. Abazajian, M. Kaplinghat, and S. Garrison-Kimmel, “Sterile neutrino dark matter bounds from galaxies of the Local Group,” *Phys. Rev. D* **89** no. 2, (2014) 025017, [arXiv:1311.0282 \[astro-ph.CO\]](#).
- [15] B. M. Roach, K. C. Y. Ng, K. Perez, J. F. Beacom, S. Horiuchi, R. Krivonos, and D. R. Wik, “NuSTAR Tests of Sterile-Neutrino Dark Matter: New Galactic Bulge Observations and Combined Impact,” *Phys. Rev. D* **101** no. 10, (2020) 103011, [arXiv:1908.09037 \[astro-ph.HE\]](#).
- [16] J. W. Foster, M. Kongsore, C. Dessert, Y. Park, N. L. Rodd, K. Cranmer, and B. R. Safdi, “Deep Search for Decaying Dark Matter with XMM-Newton Blank-Sky Observations,” *Phys. Rev. Lett.* **127** no. 5, (2021) 051101, [arXiv:2102.02207 \[astro-ph.CO\]](#).
- [17] D. Malyshev, C. Thorpe-Morgan, A. Santangelo, J. Jochum, and S.-N. Zhang, “*eXTP* perspectives for the ν MSM sterile neutrino dark matter model,” *Phys. Rev. D* **101** no. 12, (2020) 123009, [arXiv:2001.07014 \[astro-ph.HE\]](#).
- [18] A. Dekker, E. Peerbooms, F. Zimmer, K. C. Y. Ng, and S. Ando, “Searches for sterile neutrinos and axionlike particles from the Galactic halo with eROSITA,” *Phys. Rev. D* **104** no. 2, (2021) 023021, [arXiv:2103.13241 \[astro-ph.HE\]](#).
- [19] S. Ando *et al.*, “Decaying dark matter in dwarf spheroidal galaxies: Prospects for x-ray and gamma-ray telescopes,” *Phys. Rev. D* **104** no. 2, (2021) 023022, [arXiv:2103.13242 \[astro-ph.HE\]](#).
- [20] X.-D. Shi and G. M. Fuller, “A New dark matter candidate: Nonthermal sterile neutrinos,” *Phys. Rev. Lett.* **82** (1999) 2832–2835, [arXiv:astro-ph/9810076](#).
- [21] A. De Gouvêa, M. Sen, W. Tangarife, and Y. Zhang, “Dodelson-Widrow Mechanism in the Presence of Self-Interacting Neutrinos,” *Phys. Rev. Lett.* **124** no. 8, (2020) 081802, [arXiv:1910.04901 \[hep-ph\]](#).
- [22] J. M. Berryman *et al.*, “Neutrino self-interactions: A white paper,” *Phys. Dark Univ.* **42** (2023) 101267, [arXiv:2203.01955 \[hep-ph\]](#).
- [23] M. D. Astros and S. Vogl, “Boosting the production of sterile neutrino dark matter with self-interactions,” *JHEP* **03** (2024) 032, [arXiv:2307.15565 \[hep-ph\]](#).
- [24] K. Petraki and A. Kusenko, “Dark-matter sterile neutrinos in models with a gauge singlet in the Higgs sector,” *Phys. Rev. D* **77** (2008) 065014, [arXiv:0711.4646 \[hep-ph\]](#).
- [25] A. Merle, V. Niro, and D. Schmidt, “New Production Mechanism for keV Sterile Neutrino Dark Matter by Decays of Frozen-In Scalars,” *JCAP* **03** (2014) 028, [arXiv:1306.3996 \[hep-ph\]](#).
- [26] A. Adulpravitchai and M. A. Schmidt, “A Fresh Look at keV Sterile Neutrino Dark Matter from Frozen-In Scalars,” *JHEP* **01** (2015) 006, [arXiv:1409.4330 \[hep-ph\]](#).
- [27] A. Merle and M. Totzauer, “keV Sterile Neutrino Dark Matter from Singlet Scalar Decays: Basic Concepts and Subtle Features,” *JCAP* **06** (2015) 011, [arXiv:1502.01011 \[hep-ph\]](#).
- [28] R. S. L. Hansen and S. Vogl, “Thermalizing sterile neutrino dark matter,” *Phys. Rev. Lett.* **119** no. 25, (2017) 251305, [arXiv:1706.02707 \[hep-ph\]](#).
- [29] A. Datta, R. Roshan, and A. Sil, “Imprint of the Seesaw Mechanism on Feebly Interacting Dark Matter and the Baryon Asymmetry,” *Phys. Rev. Lett.* **127** no. 23, (2021) 231801, [arXiv:2104.02030 \[hep-ph\]](#).
- [30] B. J. P. Jones, “The Physics of Neutrinoless Double Beta Decay: A Primer,” in *Theoretical Advanced Study Institute in Elementary Particle Physics: The Obscure Universe: Neutrinos and Other Dark Matters*. 8, 2021. [arXiv:2108.09364 \[nucl-ex\]](#).
- [31] V. Cirigliano *et al.*, “Neutrinoless Double-Beta Decay: A Roadmap for Matching Theory to Experiment,” [arXiv:2203.12169 \[hep-ph\]](#).
- [32] M. J. Dolinski, A. W. P. Poon, and W. Rodejohann, “Neutrinoless Double-Beta Decay: Status and Prospects,” *Ann. Rev. Nucl. Part. Sci.* **69** (2019) 219–251, [arXiv:1902.04097 \[nucl-ex\]](#).
- [33] J. Schechter and J. W. F. Valle, “Neutrinoless Double beta Decay in SU(2) x U(1) Theories,” *Phys. Rev. D* **25** (1982) 2951.
- [34] A. Aranda *et al.*, “Dirac neutrinos from flavor symmetry,” *Phys. Rev. D* **89** no. 3, (2014) 033001, [arXiv:1307.3553 \[hep-ph\]](#).
- [35] E. Ma and R. Srivastava, “Dirac or inverse seesaw neutrino masses with $B - L$ gauge symmetry and S_3 flavor symmetry,” *Phys. Lett. B* **741** (2015) 217–222, [arXiv:1411.5042 \[hep-ph\]](#).
- [36] A. Addazi, J. W. F. Valle, and C. A. Vaquera-Araujo, “String completion of an SU(3)_c \otimes SU(3)_L \otimes U(1)_X electroweak model,” *Phys. Lett. B* **759** (2016) 471–478, [arXiv:1604.02117 \[hep-ph\]](#).

- [37] S. Centelles Chuliá, E. Ma, R. Srivastava, and J. W. F. Valle, “Dirac Neutrinos and Dark Matter Stability from Lepton Quarticity,” *Phys. Lett. B* **767** (2017) 209–213, [arXiv:1606.04543 \[hep-ph\]](#).
- [38] C. Bonilla, J. M. Lamprea, E. Peinado, and J. W. F. Valle, “Flavour-symmetric type-II Dirac neutrino seesaw mechanism,” *Phys. Lett. B* **779** (2018) 257–261, [arXiv:1710.06498 \[hep-ph\]](#).
- [39] J. W. F. Valle and C. A. Vaquera-Araujo, “Dynamical seesaw mechanism for Dirac neutrinos,” *Phys. Lett. B* **755** (2016) 363–366, [arXiv:1601.05237 \[hep-ph\]](#).
- [40] M. Reig, J. W. F. Valle, and C. A. Vaquera-Araujo, “Realistic $SU(3)_c \otimes SU(3)_L \otimes U(1)_X$ model with a type II Dirac neutrino seesaw mechanism,” *Phys. Rev. D* **94** no. 3, (2016) 033012, [arXiv:1606.08499 \[hep-ph\]](#).
- [41] C. Bonilla and J. W. F. Valle, “Naturally light neutrinos in *Diracon* model,” *Phys. Lett. B* **762** (2016) 162–165, [arXiv:1605.08362 \[hep-ph\]](#).
- [42] C. Bonilla, S. Centelles-Chuliá, R. Cepedello, E. Peinado, and R. Srivastava, “Dark matter stability and Dirac neutrinos using only Standard Model symmetries,” *Phys. Rev. D* **101** no. 3, (2020) 033011, [arXiv:1812.01599 \[hep-ph\]](#).
- [43] S. Weinberg, “Effective Gauge Theories,” *Phys. Lett. B* **91** (1980) 51–55.
- [44] J. Schechter and J. W. F. Valle, “Neutrino Decay and Spontaneous Violation of Lepton Number,” *Phys. Rev. D* **25** (1982) 774.
- [45] **Particle Data Group** Collaboration, S. Navas *et al.*, “Review of particle physics,” *Phys. Rev. D* **110** no. 3, (2024) 030001.
- [46] K. Abazajian, G. M. Fuller, and M. Patel, “Sterile neutrino hot, warm, and cold dark matter,” *Phys. Rev. D* **64** (2001) 023501, [arXiv:astro-ph/0101524](#).
- [47] A. Biswas and A. Gupta, “Freeze-in Production of Sterile Neutrino Dark Matter in $U(1)_{B-L}$ Model,” *JCAP* **09** (2016) 044, [arXiv:1607.01469 \[hep-ph\]](#). [Addendum: *JCAP* 05, A01 (2017)].
- [48] G. Arcadi and L. Covi, “Minimal Decaying Dark Matter and the LHC,” *JCAP* **08** (2013) 005, [arXiv:1305.6587 \[hep-ph\]](#).
- [49] A. Boyarsky, M. Drewes, T. Lasserre, S. Mertens, and O. Ruchayskiy, “Sterile neutrino Dark Matter,” *Prog. Part. Nucl. Phys.* **104** (2019) 1–45, [arXiv:1807.07938 \[hep-ph\]](#).
- [50] A. Atre, T. Han, S. Pascoli, and B. Zhang, “The Search for Heavy Majorana Neutrinos,” *JHEP* **05** (2009) 030, [arXiv:0901.3589 \[hep-ph\]](#).
- [51] **DESI** Collaboration, A. G. Adame *et al.*, “DESI 2024 VI: cosmological constraints from the measurements of baryon acoustic oscillations,” *JCAP* **02** (2025) 021, [arXiv:2404.03002 \[astro-ph.CO\]](#).
- [52] X. Luo, W. Rodejohann, and X.-J. Xu, “Dirac neutrinos and $neff$. part ii. the freeze-in case,” *Journal of Cosmology and Astroparticle Physics* **2021** no. 03, (Mar., 2021) 082. <http://dx.doi.org/10.1088/1475-7516/2021/03/082>.
- [53] X. Luo, W. Rodejohann, and X.-J. Xu, “Dirac neutrinos and $neff$,” *Journal of Cosmology and Astroparticle Physics* **2020** no. 06, (June, 2020) 058–058. <http://dx.doi.org/10.1088/1475-7516/2020/06/058>.
- [54] Z. A. Borboruah, D. Borah, L. Malhotra, and U. Patel, “Minimal Dirac seesaw dark matter,” *Phys. Rev. D* **112** no. 1, (2025) 015022, [arXiv:2412.12267 \[hep-ph\]](#).
- [55] Y. Reyimuaji and M. Abdughani, “Dirac neutrinos and dark matter within a minimal discrete symmetry model,” *Phys. Lett. B* **868** (2025) 139766, [arXiv:2408.14166 \[hep-ph\]](#).
- [56] E. Ma, P. K. Paul, and N. Sahu, “Naturally small Dirac neutrino mass and $B - L$ dark matter,” [arXiv:2601.05926 \[hep-ph\]](#).
- [57] I. P. Ivanov, M. Köpke, and M. Mühlleitner, “Algorithmic Boundedness-From-Below Conditions for Generic Scalar Potentials,” *Eur. Phys. J. C* **78** no. 5, (2018) 413, [arXiv:1802.07976 \[hep-ph\]](#).